INVOLVEMENT OF GLUTAREDOXIN-1 AND THIOREDOXIN-1 IN BETA AMYLOID TOXICITY AND ALZHEIMER'S DISEASE

Susanne Akterin[1], Richard F. Cowburn[1], Antonio Miranda-Vizuete[2,3], Alberto Jiménez[2], Nenad Bogdanovic[1], Bengt Winblad[1], and Angel Cedazo-Minguez*[1].

1. **Section of Experimental Geriatrics, Neurotec Department, Karolinska Institutet, Kliniskt Forskningscentrum (KFC), Novum, S-141 86 Huddinge, Sweden.**
2. **Department of Biosciences, Karolinska Institutet, Novum, S-141 57 Huddinge, Sweden.**
3. **Centro Andaluz de Biología del Desarrollo (CABD-CSIC), Departamento de Ciencias Ambientales, Universidad Pablo de Olavide, 41013 Sevilla, Spain.**

Running title: Glutaredoxin-1 and Thioredoxin-1 in Alzheimer's Disease

*Address correspondence to: Angel Cedazo-Minguez, PhD, Karolinska Institutet, Neurotec Department. Section of Experimental Geriatrics, Novum, KFC, plan 4. S-141 86 Huddinge, Sweden. Phone: +46 8 585 83751. Fax: +46 8 585 83880. E-mail: Angel.Cedazo-Minguez@neurotec.ki.se

Strong evidences indicate the involvement of oxidative stress in the pathology of Alzheimer's disease (AD). The amyloid β peptide (Aβ) has been implicated in both mediating this oxidative mechanism and in inducing neuronal apoptosis. Glutaredoxin-1 (GRX1) and thioredoxin-1 (TRX1) modulate the cellular redox homeostasis and inhibit the apoptosis signal-regulating kinase (ASK1). We examined the levels of GRX1 and TRX1 in AD brains and their role in the mechanisms of Aβ neurotoxicity. In AD brains we found that GRX1 levels are increased in healthy neurons and that neuronal TRX1 levels are decreased. Using SH-SY5Y cells, we demonstrated that Aβ caused an early, strong and transient oxidation of both GRX1 and TRX1. We also showed that Aβ induced apoptosis and cytosolic translocation of the Death associated protein (Daxx), a downstream protein in the ASK1 cascade. The Aβ toxicity was inhibited by Insulin Growth Factor-I (IGF-I) in a Phosphatidylinositol 3-kinase (PI3K) independent manner and also by overexpression of GRX1 or TRX1. Our results indicate that deregulation of GRX1 and TRX1 antioxidant systems could be important in AD pathogenesis and that Aβ neurotoxicity might be mediated by oxidation of GRX1 or TRX1 and subsequent activation of the ASK1 apoptotic cascade.

Alzheimer's disease (AD) is characterized by several neuropathological changes, including accumulation of intracellular neurofibrillary tangles and extracellular plaques, as well as vast synaptic and neuronal loss.

The main constituent of AD plaques is the 39-43 amino acid long, amyloid β (Aβ) peptide. Aβ deposition has been proposed as the major pathogenic event that drives AD pathology (1). The precise mechanisms leading to Aβ neurotoxicity are not fully understood, but several evidences, from both *in vitro* and *in vivo* studies, suggest that oxidative stress plays a key role (for review, see (2,3). Aβ has been shown to induce apoptosis in several paradigms (4-6), supporting the idea that the progressive cell loss seen in AD involves apoptosis. Also supporting this idea, are signs of activation of apoptosis in both transgenic models of AD and in postmortem AD brain samples (7-9).

Glutaredoxins (GRX) and thioredoxins (TRX) are endogenous antioxidant systems and key players in the balance of cellular redox homeostasis. Both proteins have two critical cysteins at their active sites, which give two different conformations, one as a

reduced dithiol (-$[SH]_2$) and the other as an oxidized disulfide (-S_2) (10). Two glutaredoxin genes (*GRX*) have been found in mammals, *GRX1* and *GRX2* (11). *GRX1* encodes GRX1, a protein that resides mainly in the cytoplasm although it can translocate into the nucleus upon certain stimuli. *GRX2* encodes two isoforms, a mitochondrial and a nuclear GRX2. When oxidized, the GRX isoforms are regenerated by reduced glutathione (GSH). The resulting oxidized glutathione (GSSG) is in turn reduced by Glutathione reductase at expense of NADPH. These molecules conform the GRX system in which GRX1 plays a prevalent role (Figure 1A) (11,12). At least two TRX isoforms have been characterized in mammals, cytosolic (TRX1) and mitochondrial (TRX2), of which TRX1 is the major redox protein. TRX are reduced by TRX reductase (TRXR) via NADPH. The TRX system is completed by a TRX peroxidase that is reduced by TRX and additionally scavenges reactive oxidative species (Figure 1B) (11,12).

In addition to their role in oxidative stress, GRX1 and TRX1 have been shown to regulate apoptosis through the Apoptosis Signaling Kinase-1 (ASK1) cascade. ASK1 is a mitogen activated protein kinase kinase kinase (MAPKKK) that is bound to the reduced state of either GRX1 or TRX1. When GRX1 or TRX1 are oxidized, ASK1 is liberated and can initiate the MAPK cascade leading to activation of c-Jun N-terminal kinase (JNK) or p38 (13-15) as well as to the translocation of Death associated protein (Daxx) from the nucleus to the cytosol (16). The exogenous administration or overexpression of GRX1 or TRX1 is protective against apoptosis, as shown in several studies (17-20). Whether this is achieved through an inhibition of the ASK1-cascade or through other ASK1-independent mechanisms is not yet clear.

The role of GRX1 and TRX1 in AD is largely unknown, but a few reports over recent years, albeit conflicting, suggest a possible involvement of these proteins in protection from AD oxidative stress. In an mRNA expression profiling study of AD hippocampal CA1 neurons, GRX1 was found to be downregulated in tangle-bearing neurons compared to normal neurons in AD brains (21). Protein levels of TRX1 have also been found to be decreased in AD brain in areas associated with AD pathology (19). In contrast, in the same study, TRXR activity was increased in AD amygdala and cerebellum. Asahina et al. (22) examined the expression of TRX1 in brains from AD patients and control subjects. In AD brain, they found intense TRX1 staining of GFAP-positive cells in the white matter, suggested to be astrocytes. The normal brain did not stain to the same extent and also no staining was found in the cortex in either AD or normal brain. The increased TRX1 expression in AD was suggested to reflect the need for increased antioxidant protection (22).

The present study aims to provide insight as to the role of GRX1 and TRX1 in AD pathology. We first investigated the expression of GRX1 and TRX1 in AD brain. Then, using human neuroblastoma SH-SY5Y cells, we analyzed the effects of Aβ on the redox states of GRX1 and TRX1, and on other antioxidant systems, specifically catalase and glutathione. Finally, we investigated the possible involvement of the ASK1-cascade in Aβ-mediated apoptosis and the possible protective effects of GRX1 and TRX1 overexpression.

MATERIAL AND METHODS

Materials - Aβ(25-35) and Aβ(35-25) were purchased from Sigma-Aldrich Sweden AB (Stockholm, Sweden). Aβ(1-42) was from U.S. Peptide (Rancho Cucamonga, CA, USA) and dissolved in serum-free minimum essential medium (MEM). Before use, the Aβ was incubated at 37 C with sporadic shaking for 48 h (4,23). Others have shown that similar preparations of Aβ(1-42) contain Aβ fibrils along with protofibrils and stable oligomers (24,25).

4-acetamido-4'-maleimidyl-stilbene-2,2'-disulfonate (AMS) was purchased from Molecular Probes (Leiden, The Netherlands). Catalase, Purpald, trichloroacetic acid (TCA), okadaic acid, PMSF, leupeptin, aprotinin, Insulin growth factor-I (IGF-I) and Ponceau

solution were from Sigma-Aldrich Sweden AB (Stockholm, Sweden). Potassium periodate was purchased from Scharlau Chemie S.A (Barcelona, Spain). LY294002 was from Calbiochem (La Jolla, CA, USA). U0126 was from Cell Signaling Technology (Beverly, MA, USA). All other chemicals were standard laboratory reagents.

Anti-GRX1 and the anti-TRX1 antibodies were from IMCO Corp. (Stockholm, Sweden). The anti-phospho-Akt antibody that detects Akt only when phosphorylated at Ser473, the anti-phospho-ERK and the anti-Lamin A antibodies were from Cell Signaling Technology (Beverly, MA, USA). The Anti-Daxx antibody was purchased from MBL Int. Corp. (MA, USA).

Post-mortem tissue and immunohistochemical analysis - Post-mortem brain material was obtained from Huddinge Brain Bank (Karolinska University Hospital, Sweden). Four definite AD brains (two males, 79 and 89 years old, two females 76 and 80 years old) and three aged-matched control (two males, 66 and 83 years old, one 85-year-old female) were used for immunohistochemistry. All brains have a post-mortem delay between 24 and 48 h. The AD cases met the clinical diagnosis of probable AD (DSM-IV criteria) as well as definite AD after CERAD neuropathological criteria (26,27).

Brain tissue blocks were fixed in buffered 4% formaldehyde and embedded in paraffin. Sections (7 μm-thick) were mounted onto Superfrost plus-glass (Menzel Braunschweig, Germany), baked at 37°C overnight, dewaxed and hydrated. Then sections were blocked for non-specific sites with Dako-protein block (X0909) (Dako Cytomation, Danmark) for 30 min prior to incubations over night at 4°C with primary antibodies (anti-GRX1 or Anti-TRX1 at 1:1000 dilutions). Then sections were incubated for 30 min with biotinylated anti-goat antibody (Vector laboratories Burlingame, UK), diluted to 5.0 μg/ml in TBS, followed by incubation in ABC-Elite HRP (Vector laboratories Burlingame, UK) for 1 h. Reactions were visualized by developing the sections in Dab (Sigma-Aldrich, Sweden). The sections were thoroughly washed in TBS between different steps. Finally, the sections were dehydrated and mounted in DPX (BDH, Poole, UK). The protocol for antibodies was repeated to assure the reproducibility of results. All sections were treated simultaneously under the same conditions. For control staining the primary antibody was omitted. For morphological recognition of the neurons hematoxylin staining was used as a background.

Cell culture - Human neuroblastoma SH-SY5Y cells were cultured in minimun essential media (MEM) with Earle's salts and L-alanine-L-glutamine, supplemented with 10% fetal bovine serum (FBS), 100 units/ml penicillin, 100 μg/ml streptomycin at 37 C in a humidified atmosphere of 5% (v/v) CO_2/air. All cell culture supplies were purchased from Gibco Invitrogen Corporation (European division, Täby, Sweden). All treatments were used under serum-free conditions. Untreated cells were used as controls.

Redox state assessment - Cells were treated with Aβ(25-35) (10 μM), Aβ(35-25) (10 μM) or Aβ(1-42) (10 μM) in MEM (pH 7.4) under serum-free conditions, for 1, 5 or 24 h. Untreated cells were used as controls. After treatment, cells were washed with ice-cold phosphate-buffered saline (PBS). To quench further disulfide exchange and preserve the post-treatment cellular oxidation state the cells were rapidly treated with 20% (w/v) TCA (28,29). Cells were harvested and collected by centrifugation (2,000 x g for 10 min) at +4 C. TCA-treated pellets were washed twice with 70% acetone and resuspended in sample buffer (62.5 mM Tris-HCl pH 7.5, 2% SDS, 10% glycerol, 0.001% bromophenol blue) with freshly added protease inhibitors (50 μg/ml PMSF, 20 μg/ml leupeptin, 20 μg/ml aprotinin). In order to dissolve the TCA-precipitates completely the samples were sonicated. Samples were stored frozen at -80 C prior to immunoblotting. Samples were boiled for 3 min at 95 C prior to incubation with the thiol-specific probe AMS overnight at 4°C. AMS covalently modifies the reduced form of the proteins, which markedly retards

electrophoretic migrations of proteins in SDS-PAGE and gives an unequivocal separation of oxidized and reduced forms of the proteins (30). Protein concentrations were determined using the bicinchoninic acid (BCA) protein assay kit (Pierce, Rockford, IL, USA). Equivalent amounts of protein were separated by SDS-PAGE using 15% or 18% acrylamide gels.

Immunoblotting - The proteins were transferred to a Protran nitrocellulose membrane (Schleicher & Schuell, Germany) after which blocking was performed in TBS-t buffer (50 mM Tris-HCl pH 7.4, 150 mM NaCl, 0.1% Tween-20) with 5% (w/v) dry milk powder. When immunoblotting using phospho-specific antibodies, blocking was performed in TBS-t buffer with 3% bovine serum albumin. Membranes were incubated with the primary antibody (anti-GRX1, anti-TRX1, anti-Daxx or anti-Lamin-A) at a dilution of 1:1000, then washed 5 x 5 min in TBS-t buffer and incubated for 1 h with horseradish peroxide (HRP)-linked anti-goat IgG (Vector Laboratories Inc., Burlingame, CA, USA), HRP-linked anti-rabbit IgG (Amersham Biosciences, Little Chalfont, England) or HRP-linked anti-mouse IgG (Amersham Biosciences, Little Chalfont, England) at a dilution of 1:2000. After other washes of 5 x 5 min signals were detected by the enhanced chemiluminiscence (ECL) system (Amersham Biosciences, Little Chalfont, England) and exposing blots to Hyperfilm (Amersham Biosciences, Little Chalfont, England). Some of the immunoblots were stripped using stripping buffer (62.5 mM Tris-HCl, pH 6.7, 2% SDS, 100 mM mercaptoethanol) at +50 C for 30 min, and then re-blotted with other antibodies.

For the experiments including IGF-I, cells were either left untreated or treated with 50 μM LY294002 and/or 5 μM U0126 for 30 minutes prior and during co-treatment with 10 μM Aβ(1-42) and 20 nM IGF-I for 5 h. Cells were then washed with PBS, harvested, and collected by centrifugation at +4 C (2,000 x g, 10 min). Cells were lysed with lysis buffer (20 mM Tris-HCl pH 7.4, 137 mM NaCl, 2 mM EDTA, 2% NP-40, 2% Triton X-100) with freshly added protease inhibitor cocktail (Sigma-Aldrich, Saint Louis, MO, USA) at a dilution of 1:500 and phosphatase inhibitors (20 mM β-glycerophosphate, 2 nM okadaic acid, 50 mM sodium flouride, 1 mM sodium orthovanadate). Lysates were stored frozen at -80 C. Immunoblotting was performed as described above using anti-phospho-Akt or anti-phospho ERK antibodies overnight at 1:1000 dilutions.

Determination of catalase activity - Catalase activity was determined as described elsewhere (31). Cells were grown in 6 cm^2 polystyrene plates. After treatment the cells were washed with ice-cold PBS, harvested and collected by centrifugation at +4 C (2,000 x g for 10 min.). Pellets were suspended in 50 mM K_3PO_4 pH 7.0, 1 mM EDTA buffer and sonicated. The cell lysates were centrifuged again at +4 C (10,000 x g for 15 min) and supernatants were saved and stored at -80 C prior to analyses. The assay utilizes the peroxidatic activity of catalase to transform methanol and hydrogen peroxide into formaldehyde. The chromagen Purpald was used to visualize the formation of formaldehyde, by measuring the absorbance at 550 nm in a plate reader spectrophotometer (Molecular Devices Spectra MAX 250). The analysis was performed in 96-well plates using formaldehyde as standard (0 – 75 μM). Care was taken during the whole sample preparation not to overheat cell lysates, since this can inactivate catalase.

Measurement of reduced Glutathione levels - A reduced glutathione (GSH) detection kit (Chemicon, Temecula, CA, USA) was used according to the manufacturer's protocol to detect GSH levels. This kit uses the dye monochlorobimane (MCB) that has a high affinity for GSH. When unbound, MCB is almost non-fluorescent, whereas GSH-bound dye fluoresces blue. Fluorescence was measured by a FLUOstar Galaxy multi-well plate reader (BMG Labtechnologies GmbH, Offenburg, Germany), the excitation and

emission wavelengths being 380 and 460 nm, respectively.

Cell viability and apoptosis measurements - Cell viability was assessed by a modified version of the MTT assay that depends on the reduction of the tetrazolium salt MTT to formazan by living cells (32). Cells were cultured in 24-well plates and treated for indicated time points with 10 μM Aβ(1-42). For the experiments including IGF-I, medium was changed to serum-free MEM and the cells were either left untreated or treated with 50 μM LY294002 and/or 5 μM U0126 for 30 minutes prior and during co-treatment with 10 μM Aβ(1-42) and 20 nM IGF-I for 5 h.

After treatment, a MTT solution (0.3 mg/ml) made in serum-free MEM without phenol red, was then added to the cells. After 1 h incubation at 37 C, the MTT solution was aspirated and isopropanol added to the cells. Aliquots were transferred to a 96-well plate and absorbances measured at 540 nm in a plate reader spectrophotometer (Molecular Devices Spectra MAX 250). Results were expressed as percentages of the respective value obtained for untreated cells at each time point.

Detection of apoptotic mono- and oligo-nucleosomes was performed using the Cell Death Detection ELISA^{PLUS} kit (Roche Diagnostics Scandinavia AB, Bromma, Sweden) according to the manufacturer's instructions. The assay is based on a quantitative sandwich ELISA using mouse monoclonal antibodies directed against DNA and histones, respectively. This renders the *in vitro* determination of apoptosis-characteristic mono- and oligonucleosomes possible. The assay was performed in 96-well plates, measured spectrophotometrically at 405 nm (Molecular Devices Spectra MAX 250).

Immunocytochemistry - Cells grown on chamber slides were fixed at 4 C in methanol for 30 min and subsequently rinsed in PBS (3 x 10 min) and permeabilised with 0.2 % Triton X-100 in PBS for 10 min. Non-specific binding of antibodies was blocked by addition of 10% goat-serum for 30 min. Cells were incubated 3 h with the anti-Daxx antibody at a 1:500 concentration. Cells were rinsed in PBS (3 x 10 min) before incubation with anti-rabbit antibody conjugated to Alexa green (1:500 dilution) in PBS + 0.3% Triton X-100 for 1 h in the dark. Finally cells were rinsed in PBS (3 x 10 min) and mounted in glycerol:PBS (1:1).

Subcellular fractionation - Nuclear and cytosolic fractions of cells were isolated using the nuclear and cytoplasmic extraction reagents kit NE-PER (Pierce, Rockford, IL, USA), according to the manufacturer's protocol. Purity of fractions was assessed by immunoblotting with anti-Lamin-A antibody, a nuclear membrane protein used as specific nuclear marker.

DNA-Constructs and transfections - The mutagenic forward primers 5'-CGAATTCGCCACCATGGATTACAAGGATGACGACGATAAGGCTCAAGAGTTTGTGAAC-3' for *GRX1* and 5'-CGAATTCGCCACCATGGATTACAAGGATGACGACGATAAGATGGTGAAGCAGATCGAG-3' for *Trx1*, and the reverse primers 5'-CGGATCCTTACTGCAGAGCTCCAATC-3' for *GRX1* and 5'-CGGATCCTTAGACTAATTCATTAAT-3' for *TRX1* were used to amplify by PCR the open reading frames (ORF) from human testis Marathon-ready™ cDNA (Clontech, Heidelberg, Germany). The forward primers introduced an *Eco*RI site followed by a Kozac sequence preceding the Flag epitope sequence and the corresponding *GRX1* or *TRX1* sequences. The reverse primers introduced a *Bam*HI site after the *GRX1* or *TRX1* stop codons. The amplified DNA was cloned into the *Eco*RI-*Bam*HI sites of the pIRESneo expression vector (Clontech, Heidelberg, Germany) and the resulting plasmids pIRES/*GRX1* and pIRES/*TRX1* were transformed into *E. coli* TOP-10 F' strain. The final constructs were purified using the midi-prep kit (QIAGEN Sciences, Maryland, USA) and confirmed by DNA sequencing.

Transient transfections were performed in 12-well plates using Lipofectamine™2000 (Gibco Invitrogen Corporation; European

division, Täby, Sweden) according to the manufacturer's instructions. SH-SY5Y cells were cultured until 90% confluence in 12-well plates and transfected with 1 μg of DNA. Cells were incubated for 24 hours before changing media for serum-free MEM with or without 10 μM Aβ(1-42) and cells were treated for 24 h prior measuring cell viability.

Statistical analyses - Analyses of differences were carried out by ANOVA followed by Fisher's protected least significant distance *post-hoc* test. A value of $p<0.05$ was considered statistically significant.

RESULTS

Grx1 and Trx1 expressions in AD brain - Figure 2 shows immunohistochemical studies of GRX1 (Figure 2A) and TRX1 (Figure 2B) expressions in frontal cortex and hippocampal CA1 regions of AD brains and aged matched controls. We found that GRX1 expression was increased in neurons of AD brains (Figure 2A). In contrast, TRX1 expression was reduced (Figure 2B). Similar results were found in slices from hippocampal dentate gyrus (data not shown).

In controls, GRX1 was localized mostly in the cytosolic compartment (Figures 2A and 3A) and was particularly visible in layer II, III and V pyramidal neurons. Generally, for control brains cortical pyramidal neurons showed more immunoreactivity than hippocampal pyramidal cells. In AD brains, hippocampal neurons showed in general more immunoreactivity than cortical neurons. In AD brains, healthy neurons as determined according to Oppenheimer's criteria, including the central position of the nucleus and the presence of a single large conspicuous nucleolus (33), displayed intensive GRX1 cytoplasmic positivity even in dendritic compartments (Figures 2A, 3B and 3D). This was in contrast to neurons with morphological features indicating neurodegeneration (changes in the shape of cell body, deformation and shifting of the nucleus to the periphery or disappearance of nucleolus), especially in hippocampal areas where a specific form of pyramidal cells degeneration (granulovacuolar degeneration) was visible (Figure 3E).

TRX1 immunoreactivity was also mainly present in the cytosol, with no differences in intensity between brain regions. TRX1 was greatly decreased in AD brains compared with controls (Figure 2B). Additionally, we found occasional positively stained astrocyte-like profiles in AD brains (asterisk in Figure 2B).

Aβ oxidizes Grx1 and Trx1 in a rapid, transient manner - GRX1 and TRX1 are redox active proteins that can have several different redox states, varying from fully reduced to fully oxidized, depending on the surrounding cellular environment. To analyze the effects of Aβ on GRX1 and TRX1 redox states, we exposed human SH-SY5Y cells for 1, 5 and 24 h to full length Aβ(1-42) (10 μM), the shorter Aβ(25-35) (10 μM) and the reverse and non-toxic form Aβ(35-25) (10 μM). Figure 4 shows the separation between the different redox states after incubation of the samples with AMS and subsequent gel electrophoresis. As determined using reducing (DTT, 10 mM) or oxidizing (H_2O_2, 1 mM) conditions, the upper band is the fully reduced and the lower the fully oxidized redox state (data not shown).

As shown in Figure 4, Aβ(1-42) (10 μM) induced an early and transient oxidation of both GRX1 and TRX1, seen at 1 h and 5 h, but not at 24 h. Aβ(25-35) (10 μM) effects were also transient, being seen only at 5 h treatment and less pronounced than those of Aβ(1-42). In contrast, the reverse peptide Aβ(35-25) (10 μM) did not induce any effect.

Effects of Aβ(1-42) on catalase and glutathione antioxidant systems - We next analyzed the effects of Aβ(1-42) on two other major cellular antioxidant systems, namely catalase and glutathione, by measuring catalase activity and levels of reduced glutathione (GSH). Catalase is an antioxidant enzyme involved in the degradation and detoxification of H_2O_2 and glutathione is the main redox buffer in the cell. SH-SY5Y cells were treated for 1, 5 and 24 h with Aβ(1-42)

(10 μM). Aβ(1-42) significantly increased catalase activity after 5 and 24 h (Figure 5A). Aβ(1-42) decreased GSH levels at 24 h with no effect at earlier time points (Fig 5B).

Aβ(1-42) induces apoptosis and Daxx translocation in SH-SY5Y cells - GRX1 and TRX1 have been shown to be regulators of the apoptosis cascade mediated by ASK1. When reduced, GRX1 and TRX1 are bound to ASK1, thereby inhibiting its activity. In contrast when they are oxidized ASK1 is free to initiate apoptosis. Aβ(1-42) has been shown to induce apoptosis in several *in vitro* models. Since we showed that Aβ(1-42) caused an early oxidation of both GRX1 and TRX1, we next analyzed the effects of Aβ(1-42) on apoptosis and the possible involvement of the ASK1 apoptotic cascade. We first studied effects on cell viability using the MTT-reduction assay. Aβ(1-42) (10 μM) inhibited MTT reduction by approximately 30 % at 2 h and by 40% at 5 and 24 h. This effect was significant with time ($p<0,0001$; ANOVA), (see Figure 6A for comparisons at each time point).

We next quantified the level of Aβ(1-42) induced apoptosis with an ELISA assay that detect cytosolic mono-and oligo-nucleosomes. Aβ(1-42) (10 μM) gave increased level of apoptosis in a time dependent manner ($p<0.0001$; ANOVA), with approximately 3 fold and 6 fold increases in mono-and oligo-nucleosomes levels after respectively 5 h after 24 h treatment, as compared to non-treated cells (Figure 6B).

In order to investigate involvement of the ASK1 cascade in the Aβ(1-42)-induced apoptosis we analyzed the Aβ(1-42) effects on Daxx translocation from the nuclei to the cytosol.

Daxx is a downstream protein in the ASK1 cascade. Activation of ASK1 induces Daxx phosphorylation and its translocation to the cytosolic compartment by a c-Jun N-terminal kinase (JNK) mediated mechanism (16,34). As shown in Figure 7A, we found that Aβ(1-42) (10 μM) induces cytosolic translocation of Daxx both at 5 and 24 h. A treatment with H_2O_2 (1 mM, 20 min) was used as a positive control for the experiment (Figure 7A).

Figure 7B shows Daxx immunoblots of nuclear and cytosolic fractions of cells treated with Aβ(1-42) (10 μM) for 5 h and H_2O_2 (1 mM) for 20 min. Loading of gels and purity of the fractions were checked respectively by Ponceau staining (Figure 7C) and immunoblotting for the nuclear specific protein Lamin A (Figure 7D). Expression of data as the ratio of cytosolic Daxx immunoreactivity / nuclear Daxx immunoreactivity, revealed that both Aβ(1-42) and the positive control H_2O_2 induced Daxx translocation (Figure 7E).

IGF-I protects against Aβ toxicity in a PI3K independently manner - IGF-I has been shown to protect against Aβ-toxicity in several cellular paradigms (35-37). This protection has been shown to involve both activation of Extracellular regulated kinase (ERK) and Phosphatidylinositol 3-kinase (PI3K) signaling pathways (37). IGF-1 has also been shown to inhibit ASK1-activity and therefore apoptosis, by a mechanism that is independent of its effects on the PI3K anti-apoptotic cascade (38). We next analysed the protective effects of IGF-I against Aβ(1-42) toxicity when ERK or PI3K anti-apoptotic pathways were inhibited. For this, we co-incubated cells with IGF-I (20 nM) and Aβ(1-42) (10 μM) with and without the specific inhibitors LY294002 (50 μM; for PI3K) and U0126 (5 μM; for MEK an upstream kinase of ERK) and then analyzed cell viability using the MTT assay. We selected a 5 h treatment since at this time point we previously showed that Aβ(1-42) induces apoptosis. The inhibitors were used in a 30 min pre-treatment and during the co-incubations with Aβ(1-42) and IGF-I. The efficiency of the inhibitors was previously checked by immunoblotting extracts of treated cells with anti-phospho-Akt (a downstream a serine/threonine kinase that is phosphorylated by PI3K) and anti-phospho-ERK antibodies. These antibodies recognize active forms of Akt and ERK. LY294002 (50 μM) and U0126 (5 μM) powerfully inhibited Akt and ERK phosphorylation respectively (Figure 8A),

without changing total expression levels of these proteins as demonstrated by immunoblotting with anti-Akt and anti-ERK antibodies (data not shown).

As shown in Figure 8B, IGF-I (20 nM) fully protected SY-SH5Y cells against Aβ(1-42) toxicity ($p<0.001$). When PI3K was blocked by LY294002 (50 μM), IGF-I was still protective ($p<0.001$). However, PI3K inhibition slightly decreased the IGF-I protection ($p<0.05$ against both controls and IGF-I treated cells) (Figure 8B). When ERK was blocked by U0126 (5 μM), IGF-I did not protect against Aβ(1-42) toxicity (Figure 8B). IGF-I / Aβ (1-42) co-treatment with simultaneous inhibition of both PI3K and ERK was more toxic than Aβ(1-42) alone ($p>0.01$).

Overexpression of Grx1 or Trx1 protects cells from Aβ toxicity - The effects of overexpression of GRX1 or TRX1 on Aβ(1-42) toxicity in SH-SY5Y cells were evaluated by studying cell viability with the MTT-assay. SH-SY5Y cells were transiently transfected with either GRX1, TRX1 or the empty vector as described in Materials and Methods. As shown in Figure 9A, GRX1 and TRX1 expression levels were significantly increased after transfection.

Then cells were incubated with 10 μM Aβ(1-42) for 24 h and cell viability determined. Treatment with Aβ(1-42) (10 μM) decreased MTT reduction by approximately 40 % in all the experiments with non-transfected and vector-transfected cells ($p<0.001$) (Figures 9B, 9C and 9D). Overexpression of TRX1 completely protected cells from Aβ(1-42) toxicity (Fig 9B). Overexpression of GRX1 also protected cells against Aβ(1-42) toxicity ($p<0.001$) but not to the same extent as seen with TRX1. Aβ(1-42) treatment in GRX1 transfected cells still decreased MTT reduction to approximately 80%, a level that was significantly different to both non-transfected and vector-transfected cells ($p<0.05$) (Fig 9C). Transfection of cells with empty vector had no effect on Aβ(1-42) toxicity (Figure 9D).

DISCUSSION

Oxidative stress is believed to have an early role in AD pathology and several reports have suggested that endogenous antioxidant systems could be affected in the disease (39-41). The GRX1 and TRX1 endogenous antioxidant systems are key players in maintaining the cellular redox status (10). In addition to their role as antioxidants, both GRX1 and TRX1 have been shown to regulate apoptosis. Reduced GRX1 and TRX1 are able to bind to ASK-1 and inhibit the pro-apoptotic MAPK cascade that leads to the activation of JNK, p38 and to the cytosolic translocation of Daxx (13-15). Despite its importance as regulators of oxidative stress and apoptosis, the role of GRX1 and TRX1 in AD is largely unknown. To provide insight of GRX1 and TRX1 in the context of AD, we addressed the issues of how GRX1 and TRX1 levels are affected in AD and what is the role of GRX1 and TRX1 in the mechanisms of Aβ neurotoxicity.

We found that GRX1 levels were increased in some neurons in both frontal cortex and hippocampal CA1 regions of AD brains. This is the first study showing expression levels of GRX1 in AD brain. In contrast, we found a reduction of neuronal TRX1 levels in the same regions. This last observation is in agreement with an earlier report by Lovell et al. (19).

The expressions of both GRX1 and TRX1 have been reported to be induced by various types of oxidative stress (for review see (42)). However, a decrease in TRX1 levels has been shown previously to occur in some diseases involving oxidative conditions, such as in neurons from spontaneously hypertensive rats (43) and in acute infection with the human immunodeficiency virus (HIV) (44). The fact that TRX1 also modulates a number of transcription factors (45) and stress-signaling kinases like ASK-1 (14) involved in apoptosis, suggests that a decrease of TRX1 may contribute to the neurodegenerative mechanisms of AD.

On the other hand, the simultaneous increase of GRX1 in neurons of AD brains may also be of importance. The fact that those

neurons overexpressing GRX1 showed an apparent normal morphology, suggests that they could possibly have a better protection against the neurodegenerative events occurring in AD. In accordance with this idea, a previous report has shown that in tangle-bearing hippocampal CA1 neurons, GRX1 mRNA levels were reduced six times as compared to normal neurons in AD brains (21).

The upregulation of GRX1 seen in AD brain could be a compensatory effect to counteract the reduction of TRX1. An inverse relation between Grx1 and Trx1 expression has been demonstrated in *Escherichia Coli,* where Grx1 levels are increased in bacteria lacking Trx1 and viceversa (46,47). In addition, a functional link between Grx and Trx expressions has been also described in yeast, where a lack of Trx causes a decrease in GSH levels which are compensated for by an increased Grx expression (48). A reduction of GSH levels has been previously demonstrated in AD brain (49), suggesting the possibility of a similar mechanism.

To further analyze the role of GRX1 and TRX1 in AD, we treated human SH-SY5Y neuroblastoma cells with different Aβ species and examined the redox status of GRX1 and TRX1. Aβ is a key molecule in AD pathology and has been shown to be neurotoxic by different mechanisms including the induction of oxidative stress (for review see (50)). We found that Aβ(1-42) caused a strong and early oxidation of both GRX1 and TRX1 that was transient with time. The intensity and early nature of these effects were in contrast with those seen for other antioxidant systems. We showed that catalase activity was increased at 5 and 24 h and levels of GSH were decreased after 24 h in response to Aβ(1-42) treatment. Our results suggest that GRX1 and TRX1 are in the first line of response against the oxidative stress caused by Aβ(1-42), at least in SH-SY5Y neuroblastoma cells. As previously discussed, the reduction in GSH levels is in accordance with earlier reports from studies with AD brain (49) and also with other *in vitro* studies (51,52). The decrease in GSH levels could further suggest that glutathione participates in the recuperation of reduced GRX1 seen at 24 h (see Figure 1). On the other hand, the recuperation of reduced TRX1 seen at 24 h, could indicate an additional upregulation of the reducing mechanisms of TRX1, ie. TRXR. In agreement with this idea TRXR levels have been shown to be increased in AD (19).

Several reports have shown that Aβ induces apoptosis in a number of different models (for review (50). On the other hand, both GRX1 and TRX1 have been shown to be negative regulators of ASK1, a stress-activated and apoptotic-inducing kinase. This negative regulation of apoptosis is dependent on the redox state of GRX1 and TRX1. ASK1 is bound to the reduced form of GRX1 and TRX1, but when GRX1 and TRX1 are oxidized ASK1 is free and can initiate apoptosis (13). In view of this, we hypothesized that the strong and quick oxidation of GRX1 and TRX1 by Aβ, albeit transient, could participate in the mechanism by which Aβ is pro-apoptotic. Indeed, we first showed that Aβ(1-42) decreased cell viability and induced apoptosis in our paradigm. We then demonstrated the involvement of the ASK1 cascade by showing that Aβ induced cytosolic translocation of Daxx at 5 and 24 h treatment. Daxx is a downstream protein in the ASK-1 pathway located in the nucleus under normal conditions (53). However, under oxidative stress, ASK1 activates JNK which phosphorylates Daxx and uncovers a nuclear export signal leading to translocation of Daxx to the cytoplasmic compartment (16,34). It has also been observed that Daxx is involved in the activation of ASK1 (54,55). In concordance with our finding that Aβ induced cytosolic translocation of Daxx, during the preparation of this manuscript, Kadowaki and collaborators showed in PC12 cells that ASK1 is required for Aβ toxicity (56). Also, in a previous report, activation of JNK, a downstream kinase of ASK1, was found to be critical for Aβ toxicity in SH-SY5Y cells (37). These evidences together with our results strongly suggest that activation of ASK1 is a key mechanism for Aβ neurotoxicity. Furthermore, since GRX1 and TRX1 when

oxidized no longer bind to ASK1 leading to its activation, it is also suggested that the strong and early oxidation of GRX1 and TRX1 by Aβ could participate in this mechanism.

To further investigate this hypothesis, we next analyzed possible strategies of protection against Aβ toxicity based in inhibiting ASK1 and on overexpressing GRX1 or TRX1. Previous studies have shown that IGF-I protects hippocampal neurons and SH-SY5Y neuroblastoma cells from Aβ toxicity (35,37). This protection has been shown to involve both activation of ERK and PI3K signaling pathways by IGF-I (37). In a recent work, Galvan et al. (38) demonstrated that IGF-I treatment inhibits the ASK1 activation seen in serum-starved L929 cells independently of the PI3K pathway. Others have also shown that ASK1 can be inhibited by Akt, a serine/threonine kinase that is activated by PI3K (57). In view of this, we analyzed the ability of IGF-I to protect against Aβ(1-42) in our model when PI3K and/or ERK pathways were blocked with the specific inhibitors, LY294002 and U0126 respectively. We showed that IGF-I completely protected against Aβ(1-42)-induced cell death. In accordance with Galvan et al. (38) inhibition of PI3K did not have a strong effect on the IGF-I protection against Aβ toxicity . IGF-I was not protective when the MEK/ERK or both PI3K/Akt and MEK/ERK pathways were inhibited. These results provide supplementary evidence that ASK1 activation is a likely important component of the mechanism of Aβ toxicity and that this toxicity may be prevented by pharmacological inhibition of ASK1.

Finally, we explored the possibility that increased levels of GRX1 or TRX1 also protect cells from Aβ toxicity. A number of reports have shown that rising levels of GRX or TRX by exogenous recombinant administration or by overexpression protects cells against several insults (17,58-60). Here we showed that increasing levels of GRX1 or TRX1 by transient transfection protect against Aβ(1-42) toxicity in SH-SY5Y cells. Taking these results together with those seen in AD brains, an increase of GRX1 in healthy neurons and the general decrease of TRX1, it is suggested that increased brain levels of GRX1 and TRX1 could be beneficial for counteracting the progression of AD pathogenesis.

In summary, we demonstrated that GRX1 levels are increased in healthy neurons while neuronal TRX1 levels are generally decreased in AD brains. We also demonstrated that Aβ(1-42) caused an early, strong and transient oxidation of both GRX1 and TRX1, and induced apoptosis by activation of the ASK1 cascade in SH-SY5Y cells. We showed that pharmacological inhibition of ASK1 by IGF-I as well as overexpression of GRX1 or TRX1 protected cells against Aβ(1-42) toxicity. I n view of this, we propose a model (Figure 10) by which Aβ toxicity could occur primarily by causing oxidative stress. The GRX1 and TRX1 endogenous antioxidant systems are in the first line of defense to try to maintain the cellular redox homeostasis. However, GRX1 and TRX1 oxidations have as a consequence the liberation and activation of ASK1 and subsequent initiation of apoptosis. Inhibition of ASK1 (by ie. IGF-I) or overexpression of GRX1 or TRX1 protects cells against the Aβ-induced damaging cascade.

Our results strongly suggest that deregulation of GRX1 and TRX1 antioxidant systems could be important in the pathogenesis of AD. Moreover, strategies leading to inhibit ASK1 or to increase GRX1 or TRX1 in neurons may have therapeutic applications for the treatment of this disease.

REFERENCES

1. Hardy, J. A., and Higgins, G. A. (1992) *Science* **256**, 184-185
2. Huang, X., Moir, R. D., Tanzi, R. E., Bush, A. I., and Rogers, J. T. (2004) *Ann N Y Acad Sci* **1012**, 153-163
3. Behl, C. (1997) *Cell Tissue Res* **290**, 471-480
4. Cedazo-Minguez, A., Popescu, B. O., Blanco-Millan, J. M., Akterin, S., Pei, J. J., Winblad, B., and Cowburn, R. F. (2003) *J Neurochem* **87**, 1152-1164
5. Loo, D. T., Copani, A., Pike, C. J., Whittemore, E. R., Walencewicz, A. J., and Cotman, C. W. (1993) *Proc Natl Acad Sci U S A* **90**, 7951-7955
6. Pereira, C., Ferreiro, E., Cardoso, S. M., and de Oliveira, C. R. (2004) *J Mol Neurosci* **23**, 97-104
7. Hwang, D. Y., Cho, J. S., Lee, S. H., Chae, K. R., Lim, H. J., Min, S. H., Seo, S. J., Song, Y. S., Song, C. W., Paik, S. G., Sheen, Y. Y., and Kim, Y. K. (2004) *Exp Neurol* **186**, 20-32
8. LaFerla, F. M., Tinkle, B. T., Bieberich, C. J., Haudenschild, C. C., and Jay, G. (1995) *Nat Genet* **9**, 21-30
9. Stadelmann, C., Deckwerth, T. L., Srinivasan, A., Bancher, C., Bruck, W., Jellinger, K., and Lassmann, H. (1999) *Am J Pathol* **155**, 1459-1466
10. Holmgren, A. (1985) *Annu Rev Biochem* **54**, 237-271
11. Holmgren, A. (2000) *Antioxid Redox Signal* **2**, 811-820
12. Das, D. K. (2004) *Antioxid Redox Signal* **6**, 405-412
13. Ichijo, H., Nishida, E., Irie, K., ten Dijke, P., Saitoh, M., Moriguchi, T., Takagi, M., Matsumoto, K., Miyazono, K., and Gotoh, Y. (1997) *Science* **275**, 90-94
14. Saitoh, M., Nishitoh, H., Fujii, M., Takeda, K., Tobiume, K., Sawada, Y., Kawabata, M., Miyazono, K., and Ichijo, H. (1998) *Embo J* **17**, 2596-2606
15. Song, J. J., and Lee, Y. J. (2003) *Biochem J* **373**, 845-853
16. Song, J. J., and Lee, Y. J. (2003) *J Biol Chem* **278**, 47245-47252
17. Daily, D., Vlamis-Gardikas, A., Offen, D., Mittelman, L., Melamed, E., Holmgren, A., and Barzilai, A. (2001) *J Biol Chem* **276**, 21618-21626
18. Murata, H., Ihara, Y., Nakamura, H., Yodoi, J., Sumikawa, K., and Kondo, T. (2003) *J Biol Chem* **278**, 50226-50233
19. Lovell, M. A., Xie, C., Gabbita, S. P., and Markesbery, W. R. (2000) *Free Radic Biol Med* **28**, 418-427
20. Andoh, T., Chock, P. B., and Chiueh, C. C. (2002) *J Biol Chem* **277**, 9655-9660
21. Ginsberg, S. D., Hemby, S. E., Lee, V. M., Eberwine, J. H., and Trojanowski, J. Q. (2000) *Ann Neurol* **48**, 77-87
22. Asahina, M., Yamada, T., Yoshiyama, Y., and Yodoi, J. (1998) *Dement Geriatr Cogn Disord* **9**, 181-185
23. Cedazo-Minguez, A., Wiehager, B., Winblad, B., Huttinger, M., and Cowburn, R. F. (2001) *Neurochem Int* **38**, 615-625
24. Hartley, D. M., Walsh, D. M., Ye, C. P., Diehl, T., Vasquez, S., Vassilev, P. M., Teplow, D. B., and Selkoe, D. J. (1999) *J Neurosci* **19**, 8876-8884
25. Ferrari, A., Hoerndli, F., Baechi, T., Nitsch, R. M., and Gotz, J. (2003) *J Biol Chem* **278**, 40162-40168
26. Bogdanovic, N., and Morris, J. H. (1995) in *Neuropathological diagnostic criteria for brain banking*, pp. 20-29, IOS press
27. Mirra, S. S., Heyman, A., McKeel, D., Sumi, S. M., Crain, B. J., Brownlee, L. M., Vogel, F. S., Hughes, J. P., van Belle, G., and Berg, L. (1991) *Neurology* **41**, 479-486
28. Frand, A. R., and Kaiser, C. A. (1999) *Mol Cell* **4**, 469-477

29. Trotter, E. W., and Grant, C. M. (2003) *EMBO Rep* **4**, 184-188
30. Kobayashi, T., Kishigami, S., Sone, M., Inokuchi, H., Mogi, T., and Ito, K. (1997) *Proc Natl Acad Sci U S A* **94**, 11857-11862
31. Johansson, L. H., and Borg, L. A. (1988) *Anal Biochem* **174**, 331-336
32. Mosmann, T. (1983) *J Immunol Methods* **65**, 55-63
33. Esiri, M., and Oppenheimer, D. R. (1996) in *Oppenheimer's diagnostic neuropathology: a practical manual*, 2nd Ed., pp. 51-77, Blackwell Science, Oxford
34. Charette, S. J., Lavoie, J. N., Lambert, H., and Landry, J. (2000) *Mol Cell Biol* **20**, 7602-7612
35. Dore, S., Kar, S., Zheng, W. H., and Quirion, R. (2000) *Pharm Acta Helv* **74**, 273-280
36. Niikura, T., Hashimoto, Y., Okamoto, T., Abe, Y., Yasukawa, T., Kawasumi, M., Hiraki, T., Kita, Y., Terashita, K., Kouyama, K., and Nishimoto, I. (2001) *J Neurosci* **21**, 1902-1910
37. Wei, W., Wang, X., and Kusiak, J. W. (2002) *J Biol Chem* **277**, 17649-17656
38. Galvan, V., Logvinova, A., Sperandio, S., Ichijo, H., and Bredesen, D. E. (2003) *J Biol Chem* **278**, 13325-13332
39. Lovell, M. A., Ehmann, W. D., Butler, S. M., and Markesbery, W. R. (1995) *Neurology* **45**, 1594-1601
40. Marcus, D. L., Thomas, C., Rodriguez, C., Simberkoff, K., Tsai, J. S., Strafaci, J. A., and Freedman, M. L. (1998) *Exp Neurol* **150**, 40-44
41. Omar, R. A., Chyan, Y. J., Andorn, A. C., Poeggeler, B., Robakis, N. K., and Pappolla, M. A. (1999) *J Alzheimers Dis* **1**, 139-145
42. Grant, C. M. (2001) *Mol Microbiol* **39**, 533-541
43. Yamagata, K., Tagami, M., Ikeda, K., Yamori, Y., and Nara, Y. (2000) *Neurosci Lett* **284**, 131-134
44. Aillet, F., Masutani, H., Elbim, C., Raoul, H., Chene, L., Nugeyre, M. T., Paya, C., Barre-Sinoussi, F., Gougerot-Pocidalo, M. A., and Israel, N. (1998) *J Virol* **72**, 9698-9705
45. Hirota, K., Matsui, M., Murata, M., Takashima, Y., Cheng, F. S., Itoh, T., Fukuda, K., and Yodoi, J. (2000) *Biochem Biophys Res Commun* **274**, 177-182
46. Miranda-Vizuete, A., Rodriguez-Ariza, A., Toribio, F., Holmgren, A., Lopez-Barea, J., and Pueyo, C. (1996) *J Biol Chem* **271**, 19099-19103
47. Prieto-Alamo, M. J., Jurado, J., Gallardo-Madueno, R., Monje-Casas, F., Holmgren, A., and Pueyo, C. (2000) *J Biol Chem* **275**, 13398-13405
48. Garrido, E. O., and Grant, C. M. (2002) *Mol Microbiol* **43**, 993-1003
49. Ramassamy, C., Averill, D., Beffert, U., Bastianetto, S., Theroux, L., Lussier-Cacan, S., Cohn, J. S., Christen, Y., Davignon, J., Quirion, R., and Poirier, J. (1999) *Free Radic Biol Med* **27**, 544-553
50. Small, D. H., Mok, S. S., and Bornstein, J. C. (2001) *Nat Rev Neurosci* **2**, 595-598
51. Cecchi, C., Latorraca, S., Sorbi, S., Iantomasi, T., Favilli, F., Vincenzini, M. T., and Liguri, G. (1999) *Neurosci Lett* **275**, 152-154
52. Cardoso, S. M., and Oliveira, C. R. (2003) *Free Radic Res* **37**, 241-250
53. Kiriakidou, M., Driscoll, D. A., Lopez-Guisa, J. M., and Strauss, J. F., 3rd. (1997) *DNA Cell Biol* **16**, 1289-1298
54. Chang, H. Y., Nishitoh, H., Yang, X., Ichijo, H., and Baltimore, D. (1998) *Science* **281**, 1860-1863
55. Ko, Y. G., Kang, Y. S., Park, H., Seol, W., Kim, J., Kim, T., Park, H. S., Choi, E. J., and Kim, S. (2001) *J Biol Chem* **276**, 39103-39106
56. Kadowaki, H., Nishitoh, H., Urano, F., Sadamitsu, C., Matsuzawa, A., Takeda, K., Masutani, H., Yodoi, J., Urano, Y., Nagano, T., and Ichijo, H. (2005) *Cell Death Differ* **12**, 19-24

57. Kim, A. H., Khursigara, G., Sun, X., Franke, T. F., and Chao, M. V. (2001) *Mol Cell Biol* **21**, 893-901
58. Takagi, Y., Mitsui, A., Nishiyama, A., Nozaki, K., Sono, H., Gon, Y., Hashimoto, N., and Yodoi, J. (1999) *Proc Natl Acad Sci U S A* **96**, 4131-4136
59. Kenchappa, R. S., Diwakar, L., Boyd, M. R., and Ravindranath, V. (2002) *J Neurosci* **22**, 8402-8410
60. Bai, J., Nakamura, H., Hattori, I., Tanito, M., and Yodoi, J. (2002) *Neurosci Lett* **321**, 81-84

FOOTNOTES

Acknowledgements - This research was supported by grants from the following Swedish foundations: Hjärnfonden (Swedish Brain Foundation), Loo and Hans Ostermans stiftelse, Gun och Bertil Stohnes Stiftelse, Karolinska Institutets fund for geriatric research, Åke Wiberg foundation, Svenska Lundbeck stiftelsen, Demensförbundet, Alzheimerfonden, Lars Hiertas minnesstiftelse, Gamla Tjänarinnor foundation and Insamlingsstiftelsen för Alzheimer och demensforskning. A. M-V. was supported by Swedish Medical Research Council (Projects 03P-14096, 03X-14041, and 13X-10370). A. J. was supported by a postdoctoral fellowship EX2003-0390 from the Spanish Ministerio de Educacion, Cultura y Deporte. We thank Inga Volkman and Anna Sandebring for their technical assistance.

FIGURE LEGENDS

Figure 1. Glutaredoxin (A) and Thioredoxin (B) sytems.

Figure 2. Expression of Grx1 and Trx1 in AD brains. Immunostaining of GRX1 (A) and TRX1 (B) in frontal cortex and hippocampal CA1 regions from one AD brain (female, 80 years old) and one control brain (female, 83 years old). GRX1 expression was increased while TRX1 expression was decreased in neurons of AD brains. In AD brains, an occasional increase in immunoreactivity was found in astrocyte-like profiles for TRX1 (asterisk) in all regions analysed. Similar expression patterns were seen in the other brains studied.

Figure 3. Grx1 immunoreactivity is increased in healthy neurons in AD. Staining of individual neurons with the anti-GRX1 antibody in frontal cortex from control (A) and AD brains (B) as well as in hippocampal CA1 from control (C) and AD brains (D, E). As shown in Figures 3B and 3D the neurons with high immunoreactivity of GRX1 in AD brains showed a normal morphology (shape, central nucleus, single nucleolus). In contrast, signs of neurodegeneration such us displayed nucleus and granulovacuolar degeneration were found in AD brain neurons with low GRX1 expression (Figure 3E). Bar = 10 μm.

Figure 4. Effects of Aβ on the redox states of Grx1 and Trx1. GRX1 and TRX1 immunoblots of lysates from cells treated with 10 μM of Aβ(1-42), Aβ(25-35) or the reverse Aβ(35-25) for 1, 5 and 24 h, as well as untreated cells (C). AMS was added to the samples to separate the different redox forms. Three individual experiments gave similar results.

Figure 5. Effects of Aβ(1–42)on catalase activity (A) and on GSH levels (B). Cells were treated for 1, 5 h or 24 h with 10 μM Aβ(1-42). Untreated cells were used as controls (C). Data are mean ± S.E.M. of 6 experiments expressed as ratio of values for untreated cells. Statistical

analysis of the results was carried out using ANOVA followed by Fisher's PLSD post-hoc test. *, $p < 0.05$.

Figure 6. Aβ(1–42) reduces cell viability and induces apoptosis in SH-SY5Y cells.
A, Effects of 10 μM Aβ(1-42) on MTT reduction. Cells were treated for 1, 2, 5, 10 or 24 h. Data are expressed as percentage of values in untreated cells and represent the mean ± S.E.M of 4 experiments performed in triplicate.
B, Effects of 10 μM Aβ(1-42) on apoptosis. Cells were treated for 1, 5 or 24 h. Data are expressed as ratio with values in untreated cells and represent the mean ± S.E.M of 3 experiments performed in triplicate.
Statistical analysis of the results was carried out using ANOVA followed by Fisher's PLSD post-hoc test. *, $p < 0.05$; ***, $p<0.001$.

Figure 7. Aβ(1-42) induces Daxx translocation in SH-SY5Y cells. A, micrographs of SH-SY5Y cells that were untreated (Control), treated with 1 mM H_2O_2 for 20 min or with 10 μM Aβ(1-42) and then stained for Daxx. In untreated cells, Daxx immunofluorescence was concentrated mainly in the nuclei. Both Aβ(1-42) and H_2O_2 treatments induced translocation of Daxx and immunfluorescence was seen in the cytosolic projections of SH-SY5Y cells. Some examples are indicated by arrows.
Figure 7B shows Daxx immunoblots of nuclear and cytosolic fractions of cells treated with Aβ(1-42) (10 μM) for 5 h and H_2O_2 (1 mM) for 20 min. Untreated cells were used as controls (C). Two pools of control cells and two of Aβ(1-42) treated cells were analysed.
Figure 7C shows a Lamin A immunoblot of nuclear and cytosolic fractions. Lamin A immunoreactivity was only present in the nuclear fraction. Figure 7D shows the same gels shown on Figure 7A stained with Ponceau solution.
Figure 7E shows data expressed as the ratio of cytosolic Daxx immunoreactivity / nuclear Daxx immunoreactivity.

Figure 8. IGF-1 protects against Aβ toxicity in a PI3K independently manner. A, Immunoblotting for phospho-Akt or phospho-ERK in SH-SY5Y cells after the following treatments: untreated, Aβ(1-42) (10 μM), IGF-I (20 nM) or IGF-I (20 nM) together with Aβ(1-42) (10 μM) with and without the specific inhibitors LY294002 (50 μM; for PI3K) and U0126 (5 μM; for MEK/ERK). The inhibitors were used in a 30 min pre-treatment and during the incubations with the different conditions for 5 h.
B, Effects of IGF-I (20 nM) on Aβ(1-42) (10 μM) induced decrease of cell viability. C = untreated cells; Aβ = Aβ(1-42) (10 μM, 5 h); Aβ + IGF-I = co-incubation of Aβ(1-42) (10 μM) and IGF-I (20 nM) for 5 h; LY= LY294002 (50 μM); U0= U0126 (5 μM). Inhibitors LY and UO were used in a 30 min pre-treatment and during the co-incubations with Aβ(1-42) and IGF-I. Data are expressed as percentage of values for untreated cells and represent the mean ± S.E.M of 3 experiments performed in triplicate.
Statistical analysis of the results was carried out using ANOVA followed by Fisher's PLSD post-hoc test. *, $p < 0.05$; ***, $p<0.001$ against untreated cells. ¶¶, $p < 0.01$; ¶¶¶, $p<0.001$ against Aβ treated cells. #, $p < 0.05$; ###, $p<0.001$ against Aβ+IGF-I treated cells.

Figure 9. Overexpression of Grx1 or Trx1 protects cells from Aβ toxicity. A, Immunoblots of GRX1 and TRX1 expression in non-transfected (NT), pIRES vector (VT), pIRES/GRX1 (GRX1T)T and pIRES/TRX1 (TRX1T) transiently transfected human SH-SY5Y neuroblastoma cells.

B, C and D, Effects of Aβ(1-42) (10 μM, 24 h) on cell viability in GRX1 transfected (B), TRX1 transfected (C) and vector transfected (D) cells.
Data represent the mean values from 7 to 9 wells ± S.E.M. and are expressed as percentage of values for untreated cells values in the respective experiments.
Statistical analysis of the results was carried out using ANOVA followed by Fisher's PLSD post-hoc test. *, $p<0.05$; ***, $p<0.001$ against untreated cells. ###, $p<0.001$ against Aβ(1-42) treated cells.

Figure 10. Schematic representation of the involvement of Grx1 and Trx1 on Aβ(1-42) toxicity. Oxidative stress caused by Aβ induces a strong early oxidation of GRX1 and TRX1. As a consequence, the inhibitory bindings of GRX1 and TRX1 to ASK1 are disrupted and ASK1 is liberated and initiates an apoptosis cascade. Treatment with IGF-I or overexpression of GRX1 or TRX1 inhibits ASK1 and protects cells against the Aβ toxicity.

FIGURE 1

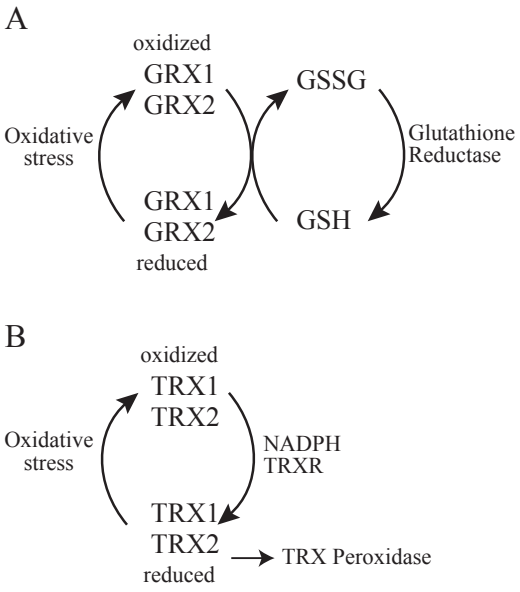
A
oxidized
GRX1
GRX2
GSSG
Oxidative
stress
Glutathione
Reductase
GRX1
GRX2
GSH
reduced
B
oxidized
TRX1
TRX2
Oxidative
stress
NADPH
TRXR
TRX1
TRX2
TRX Peroxidase
reduced

FIGURE 2

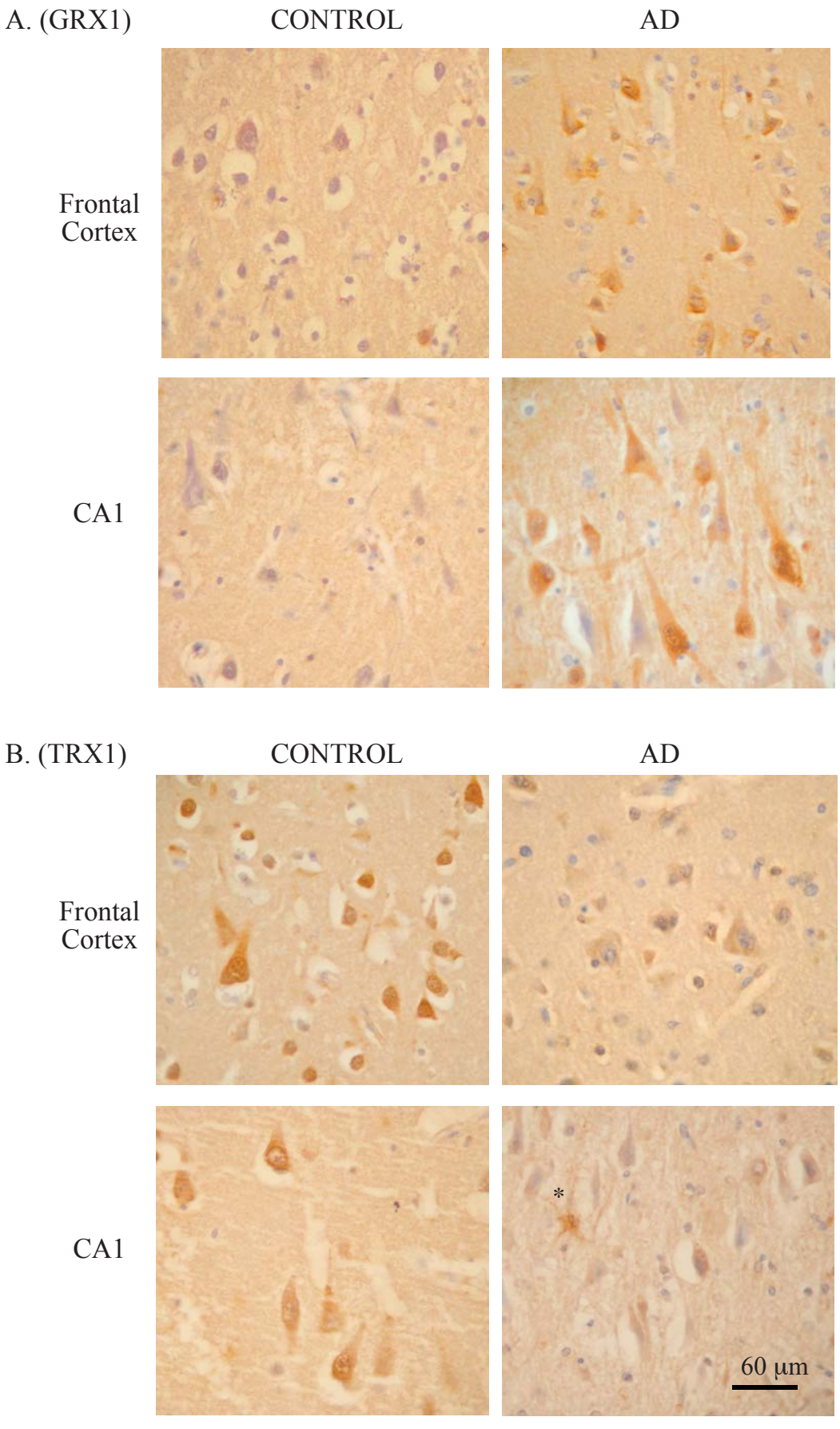
A. (GRX1)
CONTROL
AD
Frontal Cortex
CA1
B. (TRX1)
CONTROL
AD
Frontal Cortex
CA1
*
60 μm

FIGURE 3

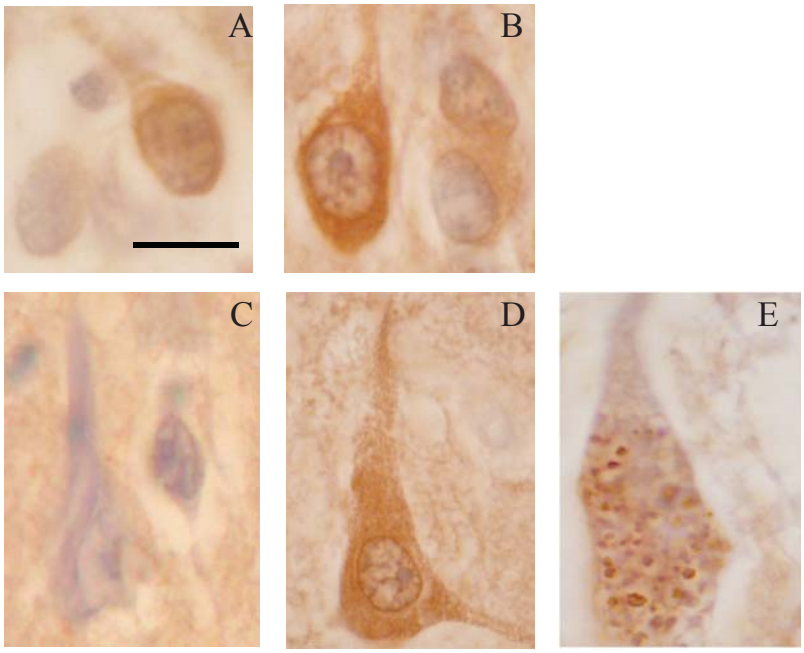

FIGURE 4

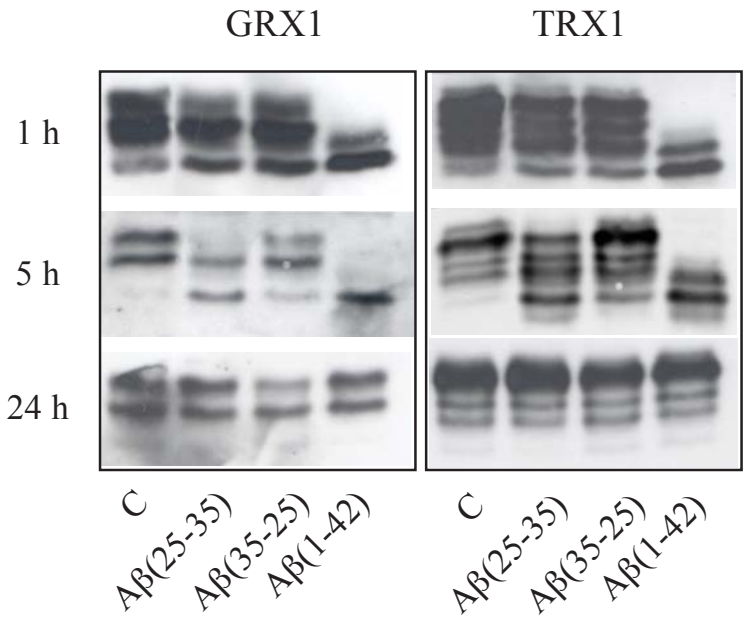
GRX1
TRX1
1 h
5 h
24 h
C
Aβ(25-35)
Aβ(35-25)
Aβ(1-42)
C
Aβ(25-35)
Aβ(35-25)
Aβ(1-42)

FIGURE 5

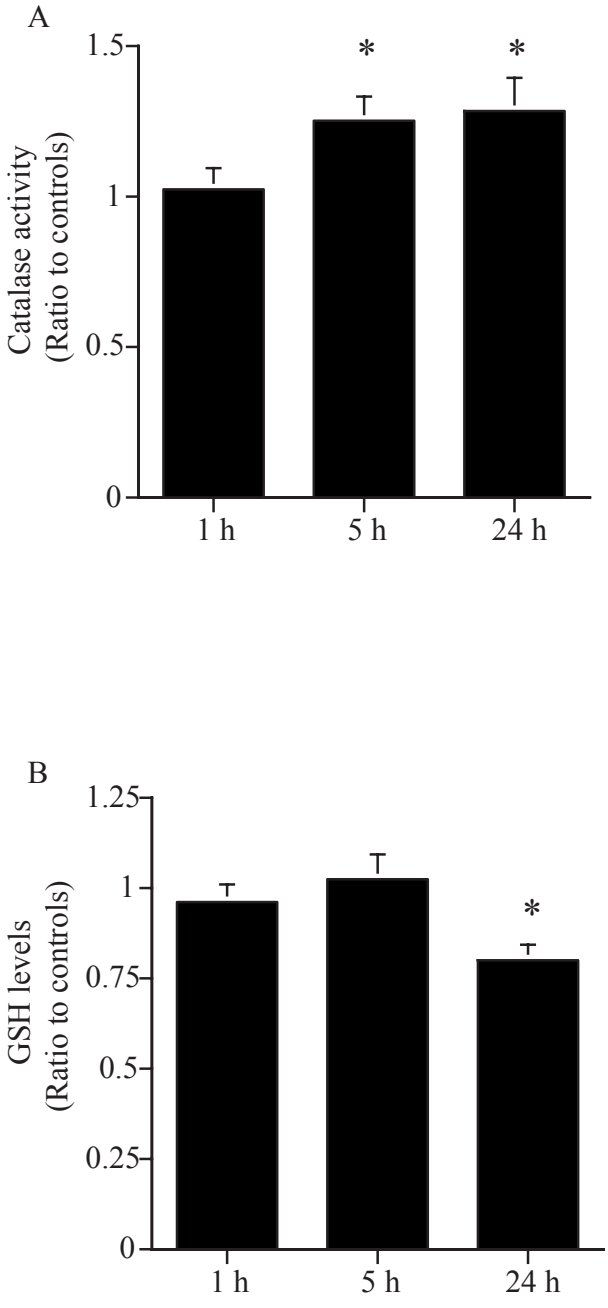
A
Catalase activity
(Ratio to controls)
1.5
1
0.5
0
*
*
1 h
5 h
24 h
B
GSH levels
(Ratio to controls)
1.25
1
0.75
0.5
0.25
0
*
1 h
5 h
24 h

FIGURE 6

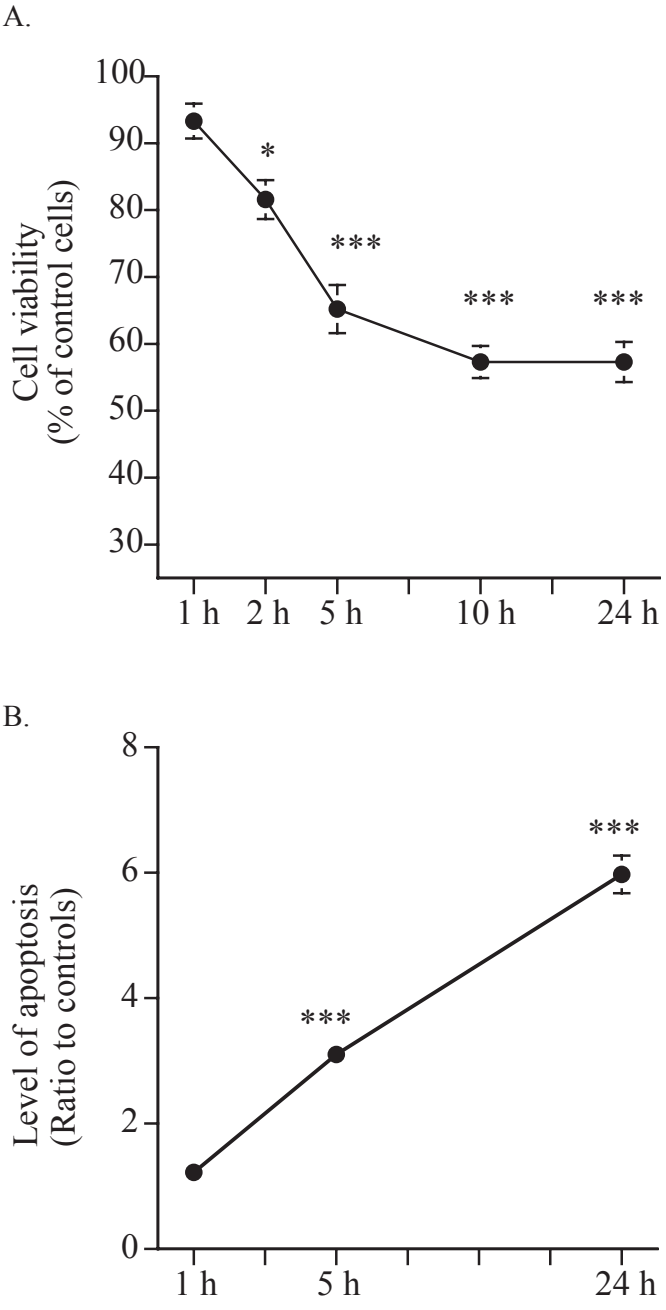
A.
Cell viability
(% of control cells)
100
90
80
70
60
50
40
30
*
***
***
***
1 h
2 h
5 h
10 h
24 h
B.
Level of apoptosis
(Ratio to controls)
8
6
4
2
0
***
***
1 h
5 h
24 h

FIGURE 7

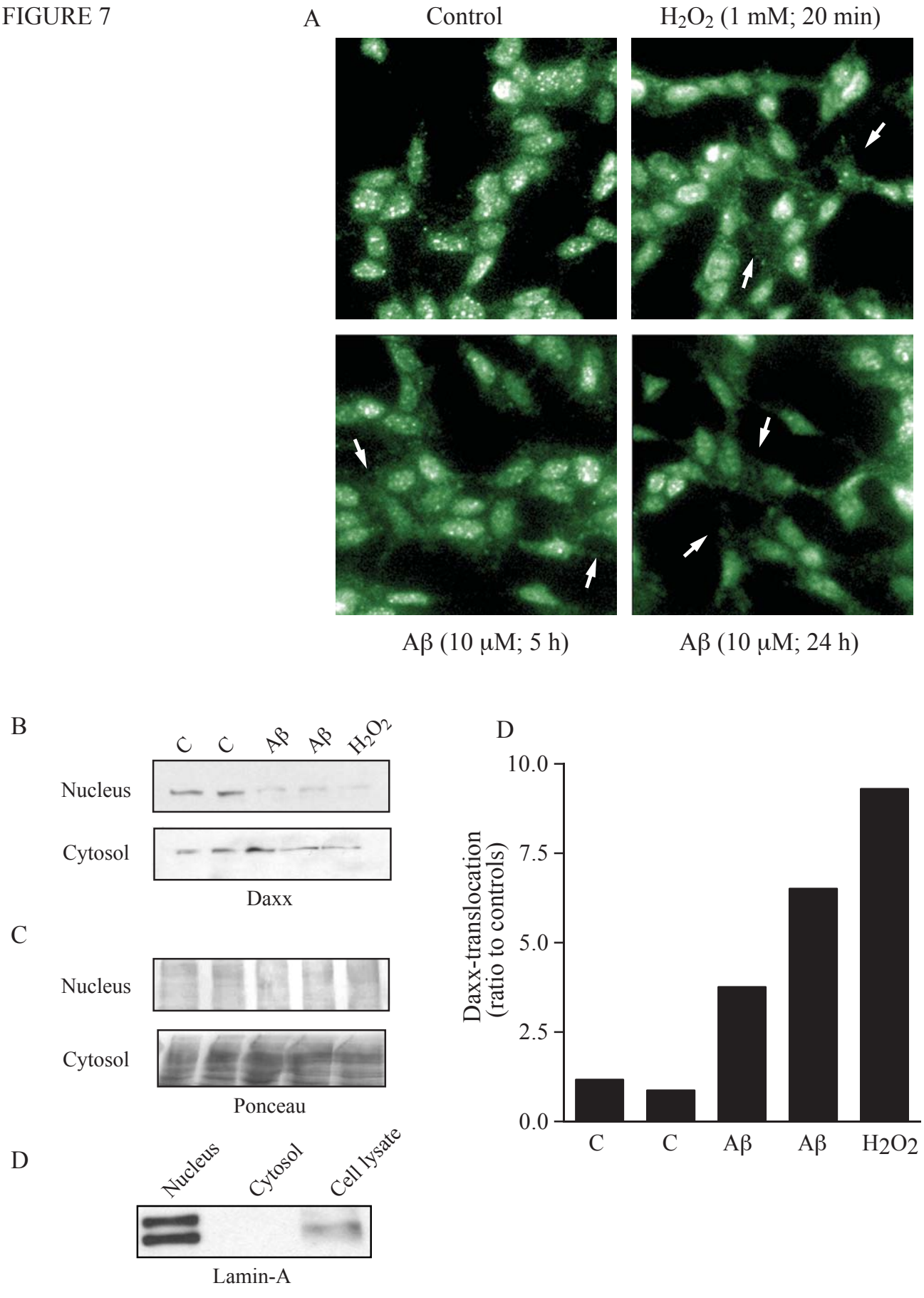
A
Control
H_2O_2 (1 mM; 20 min)
Aβ (10 μM; 5 h)
Aβ (10 μM; 24 h)
B
C C Aβ Aβ H_2O_2
Nucleus
Cytosol
Daxx
C
Nucleus
Cytosol
Ponceau
D
Nucleus Cytosol Cell lysate
Lamin-A
D
Daxx-translocation (ratio to controls)
10.0
7.5
5.0
2.5
0.0
C C Aβ Aβ H_2O_2

FIGURE 8

A.

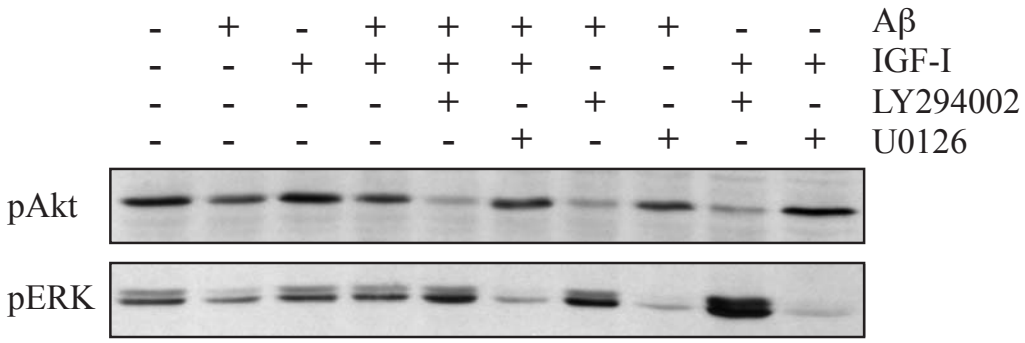
- + - + + + + + - - Aβ
- - + + + + - - + + IGF-I
- - - - + - + - + - LY294002
- - - - - + - + - + U0126
pAkt
pERK

B.

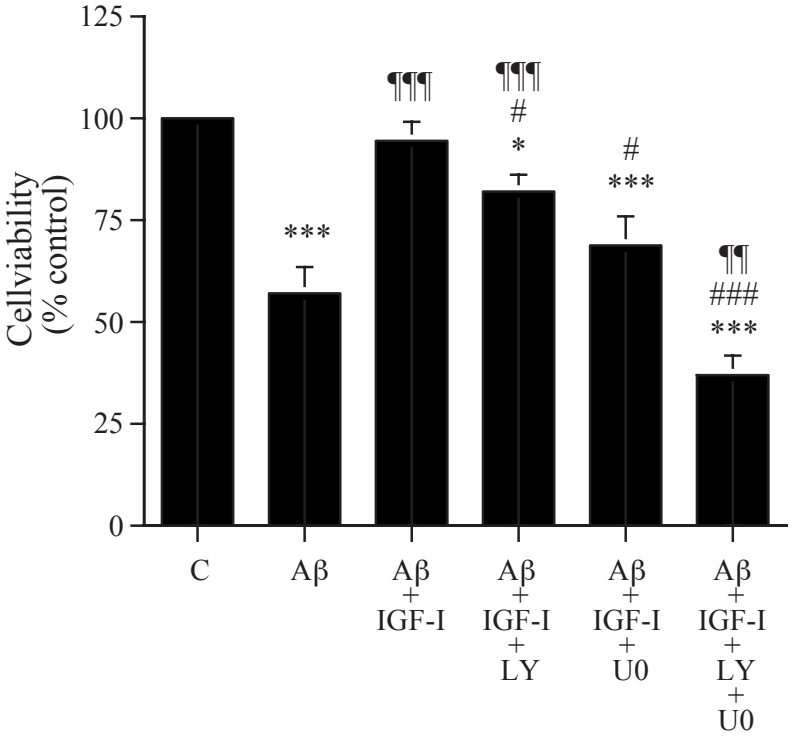
Cellviability (% control)
125
100
75
50
25
0
***
¶¶¶
¶¶¶ # *
# ***
¶¶ ### ***
C
Aβ
Aβ + IGF-I
Aβ + IGF-I + LY
Aβ + IGF-I + U0
Aβ + IGF-I + LY + U0

FIGURE 9

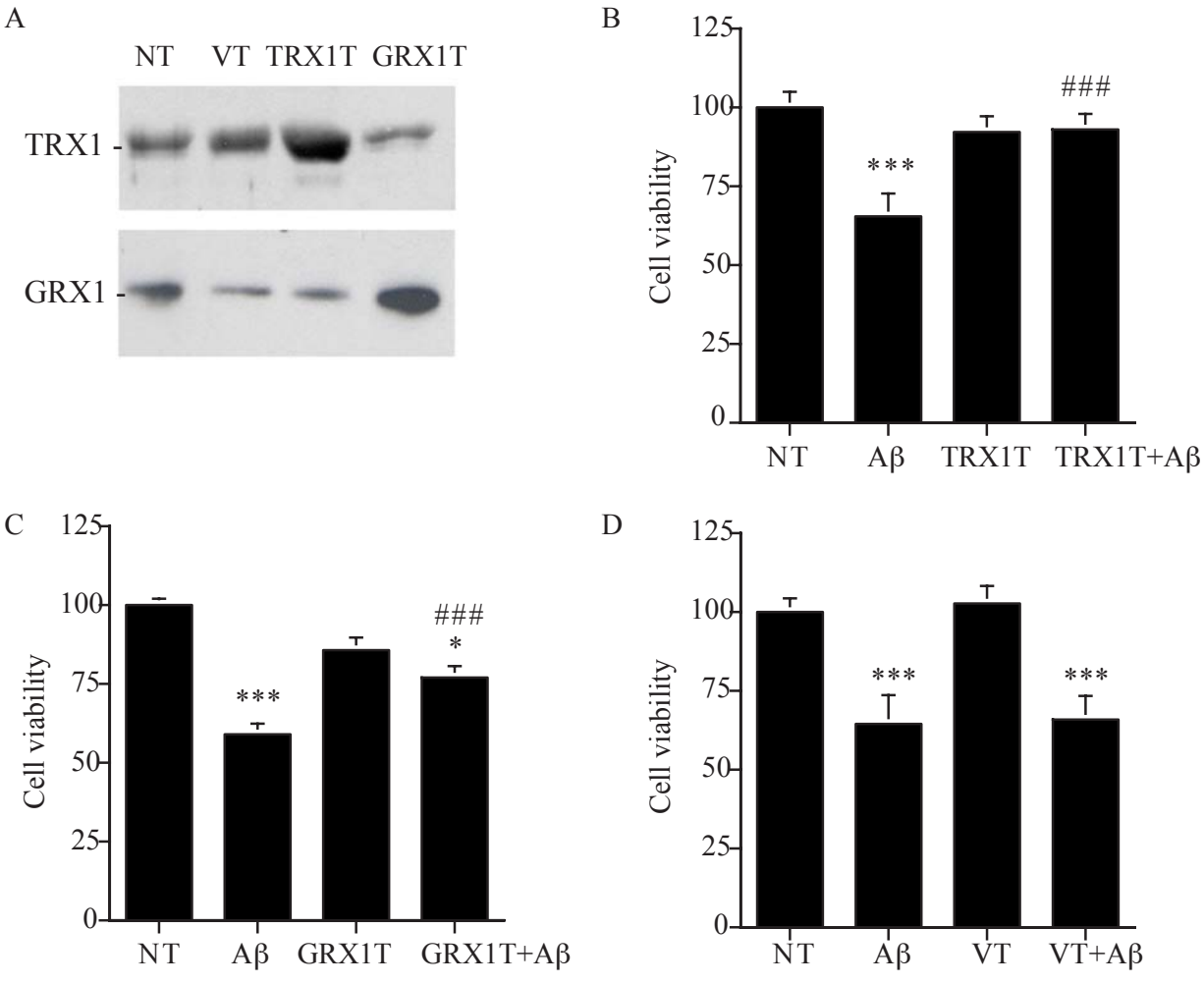
A
NT
VT
TRX1T
GRX1T
TRX1
GRX1
B
Cell viability
125
100
75
50
25
0
***
###
NT
Aβ
TRX1T
TRX1T+Aβ
C
Cell viability
125
100
75
50
25
0
***
###
*
NT
Aβ
GRX1T
GRX1T+Aβ
D
Cell viability
125
100
75
50
25
0
***
***
NT
Aβ
VT
VT+Aβ

FIGURE 10

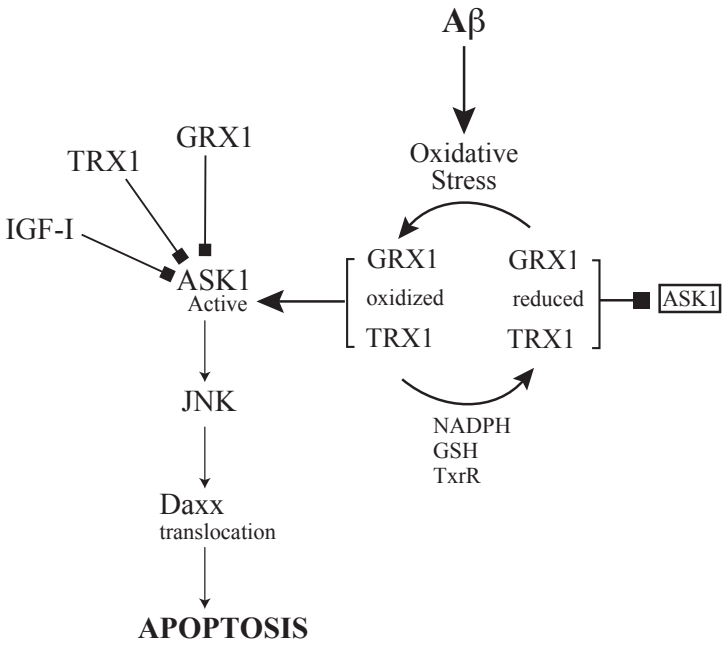
Aβ
Oxidative Stress
GRX1
TRX1
IGF-I
ASK1
Active
GRX1
oxidized
TRX1
GRX1
reduced
TRX1
ASK1
JNK
NADPH
GSH
TxrR
Daxx
translocation
APOPTOSIS